



## Effect of Ti doping on spin injection and relaxation in few-layer graphene



Bing Zhao<sup>a</sup>, Xiaoguang Xu<sup>a,\*</sup>, Le Wang<sup>b,\*\*</sup>, Juan Li<sup>a</sup>, Ziyu Zhang<sup>a</sup>, Pengfei Liu<sup>a</sup>, Qi Liu<sup>a</sup>, Zhicheng Wang<sup>a</sup>, Yong Jiang<sup>a</sup>

<sup>a</sup> School of Materials Science and Engineering, University of Science and Technology Beijing, Beijing, 100083, China

<sup>b</sup> Department of Physics, Renmin University of China, Beijing, 100872, China

### ARTICLE INFO

#### Article history:

Received 15 September 2017

Received in revised form

10 November 2017

Accepted 11 November 2017

Available online 12 November 2017

### ABSTRACT

We demonstrate the spin filtering effect in Co|MgO|TiO<sub>x</sub>|graphene junctions and a large negative spin polarization in graphene at room temperature. By systematically introducing Ti (TiO<sub>x</sub>) clusters to the exfoliated few-layer graphene, we confirm that the Ti (TiO<sub>x</sub>) clusters will increase the charged impurity scattering and lead to a decreased momentum scattering time and an abnormal Gaussian broadening effect. However, the spin relaxation mechanism is not significantly affected, indicating that the spin relaxation mechanism of graphene will not be affected by the atomic-scale Ti (TiO<sub>x</sub>) clusters induced charged impurity scattering.

© 2017 Elsevier Ltd. All rights reserved.

### 1. Introduction

Graphene [1–6], a promising material for spintronics, has gained a lot attention due to the low intrinsic spin orbit coupling [7] and weak hyperfine interaction [8,9]. Prior studies were mainly focused on monolayer, bilayer and trilayer graphene. It is very difficult to explore the intrinsic spin relaxation mechanism of graphene in these 1–3 layer graphene because of the gauge fields associated with strain, topological defects and ripples [6,10,11]. Whereafter, Van Wees et al. demonstrated a reduced spin flip rate with the number of graphene layers. It was also found that the change in the band structure, the screening effect and phonons have little influence on the spin diffusion and spin relaxation [12]. Theoretical and experimental works indicate that graphene can exhibit strong extrinsic spin orbit coupling (SOC) induced by proximity to impurities [13–15] or metal substrates [16]. Recently, a van de Waals heterostructure [17,18] composed of atomically thin graphene and semiconductor transition metal dichalcogenides (TMDCs) [19–21] shows the possibility to manipulate spins by a spin based field-effect transistor [22,23]. But the proposed origin, SOC enhancement in graphene or (and) spin absorption in TMDCs, is still in controversial and remains elusive [24–30].

To explore the mechanism of the spin relaxation, one usually needs to use two different physical processes to extract the spin relaxation time  $\tau_s$  and the momentum relaxation time  $\tau_p$  [31,32]. The Hanle effect measurement is traditionally performed to extract the spin relaxation time  $\tau_s$ , while the momentum relaxation time  $\tau_p$  is electrically determined using Boltzmann transport theory [32]. Generally, the Elliot-Yafet (EY) mechanism [33–35], for which  $\tau_s$  is proportional to  $\tau_p$ , and the D'yakonov-Perel (DP) mechanism [35], for which  $\tau_s$  is proportional to  $1/\tau_p$ , are applied to explain experimental spin relaxation in graphene. However, there are many possible sources of spin relaxation including charged impurity (CI) scatterings [32,36,37], Rashba SOC due to adatoms [13,38], ripples [34,39], edge effects [40] and resonant scattering [41,42]. Determining the origin of the spin relaxation in graphene is still an important challenge [6]. As we know, it is impossible to extract the real spin relaxation time  $\tau_s$  because of the conductance mismatch [2,43]. To alleviate the absorption of the spins that have been injected into graphene, tunnel barriers are usually inserted between the ferromagnetic materials and graphene [43]. In the early works, the oxide was directly deposited on graphene and it was nonuniform [5]. This made the tunnel barrier almost transparent [44]. Kawakami's group introduced a Ti/TiO<sub>x</sub> wetting layer yielding a more homogeneous MgO layer [45] and demonstrated that the barrier was indeed a schottky one [46]. But the impact of Ti or TiO<sub>x</sub> on the properties of graphene is still an open question [47]. Many works have proved that the substrates and roughness are not the

\* Corresponding author.

\*\* Corresponding author.

E-mail addresses: [xgxu@ustb.edu.cn](mailto:xgxu@ustb.edu.cn) (X. Xu), [le.wang@ruc.edu.cn](mailto:le.wang@ruc.edu.cn) (L. Wang).

limited factors which affect the spin relaxation in graphene [31,48]. But the contacts as spin injector (detector) and contaminations on the graphene channel are indeed the predominate ones in the current regime of spin lifetimes (~1 ns) [49]. Some papers have shown that Cu, Au and Ag clusters on the graphene channel can improve the SOC of the channel apparently [15,50]. So is there any effect on the spin relaxation by using Ti/TiO<sub>x</sub> as a barrier or some remnants introduced onto the channel unintentionally? A systematic investigation on the role of the Ti (TiO<sub>x</sub>) in spin relaxation of graphene has been lacking.

In this work we systematically introduce Ti on few-layer graphene (FLG) spin valves as a wetting layer and remnants on the graphene channel, respectively. For the first time we observe an inverted sign of the signal and the spin filtering effect in the Co|MgO|TiO<sub>x</sub>|Gr junctions with a contact resistance higher than 4 kΩ and the contact resistance area product R<sub>c</sub>A = 2.7 kΩμm<sup>2</sup>. Moreover, we find that the doping with Ti (TiO<sub>x</sub>) causes large shifts of the charge neutrality point, indicating a significant charge transfer to the graphene layer and an increased momentum scattering, accompanied by the abnormal Gaussian broadening effects. However the Ti (TiO<sub>x</sub>) induced charged impurity scattering effect on the spin transport mechanism is limited.

### 2. Experimental details

Graphene flakes (Highly Oriented Pyrolytic Graphite, grade ZYA) with 5–10 atom layers were mechanically transferred onto the n-doped 300 nm SiO<sub>2</sub>/Si substrate. A Back gate voltage was applied to the Si substrate to tune the carrier concentration in graphene. Electrical contacts to the graphene were made using standard electron beam lithography. A subsequent e-beam evaporation of 1 nm TiO<sub>2</sub>, 2.5 nm MgO, and 65 nm Co produce the spin sensitive ferromagnetic electrodes with tunneling contacts. The TiO<sub>2</sub> barrier was prepared by a twofold evaporation of 5 Å of Ti and in-situ oxidation in an oxygen atmosphere. The electrodes were then capped with 20 nm Au. Typically the contact resistance is in the range of 2–6 kΩ (except as otherwise noted), which is enough to tackle the conductivity mismatch problem compared to the square resistance of FLG [51]. The samples were annealed at 270 °C for 3 h in N<sub>2</sub>/H<sub>2</sub>, and no further annealing steps are applied. All the measurements are performed at room temperature using a DC current (10–30 μA) source Keithley 2400, while the voltage signal is measured by Keithley 2182 A.

### 3. Results and discussion

Charge and spin transport measurements are performed at room temperature. Fig. 1(a) is the schematic diagram of non-local measurement technology. Fig. 1(b) shows the optical microscope image of FLG. Atomic force microscope (AFM) images of the FLG before and after Ti-deposition are presented in Fig. 1(c) and (d). It is obvious that dots on the surface of Ti-decorated FLG are evenly dispersed. Notably, the adhesive residues usually gather together rather than homogeneously distribute on the graphene as marked in Fig. 1(e). Moreover, the roughness of graphene increases with the Ti (TiO<sub>x</sub>) thickness as listed in Table 1. Therefore, the Ti-decorations are evenly dispersed on the FLG.

Fig. 2 presents the spin signal of a lateral spin valve with FLG channel. Fig. 2(a) shows a typical spin signal, and Fig. 2(b) presents the corresponding Hanle curves (R<sub>nl</sub>) for parallel (P) and antiparallel (AP) alignment of the magnetic moments in the injector and detector magnetic electrodes. The variation in Hanle curves R<sub>nl</sub> can be well described by the expression Eq. (1) which includes the contributions of spin diffusion, precession and dephasing [51,52].

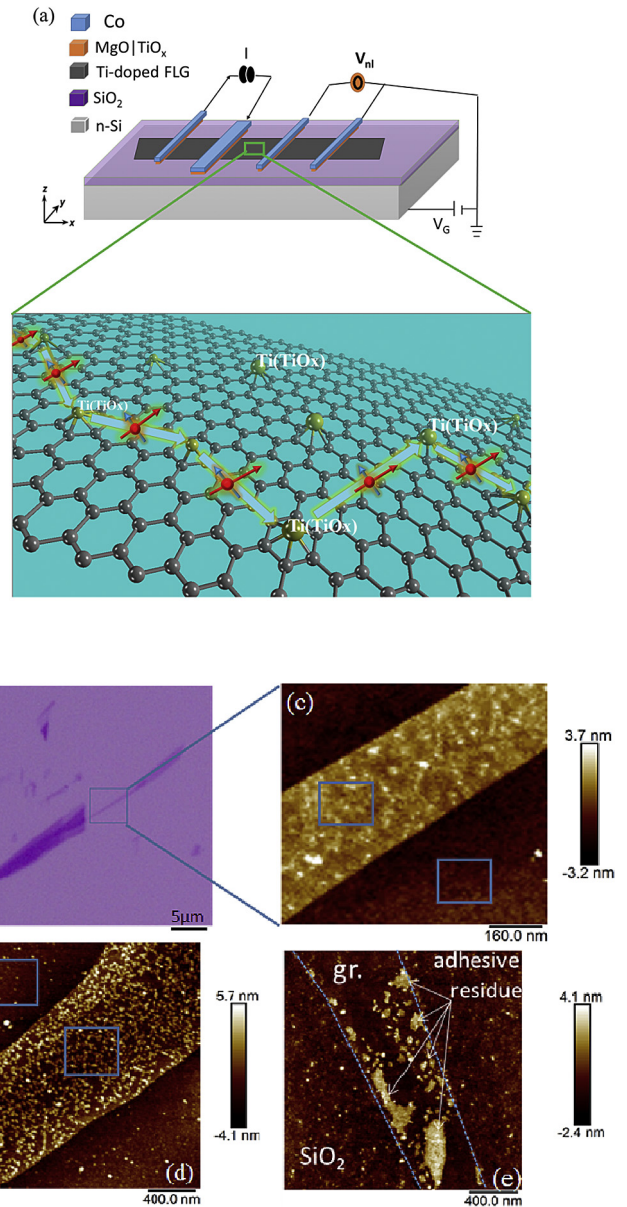


**Fig. 1.** (a) Schematic representation of the nonlocal measurement and back-gate arrangement. The schematic diagram of the enlarged Ti-doped FLG illustrates the pure spin current transport mechanism in the channel scattered by the Ti (TiO<sub>x</sub>) clusters (b) Optical microscope photograph. (c) AFM image of graphene of the marked area in (a). (d) AFM image of Ti-evenly-decorated graphene. (e) Adhesive residues on graphene. (A colour version of this figure can be viewed online.)

$$\Delta R_{nl} = \pm \frac{p_i p_d D_s R_{sq}}{W} \int_0^\infty \frac{1}{\sqrt{4\pi D_s t}} e^{-\frac{l^2}{4D_s t}} \cos(\omega_l t) e^{-\frac{t}{\tau_s}} dt \quad (1)$$

where ± sign represents the parallel (antiparallel) magnetization state, W is the width of the graphene channel, R<sub>sq</sub> is the square resistivity, p<sub>i</sub> and p<sub>d</sub> are the spin polarizations for the injector and the detector separated at a length of L. D<sub>s</sub> and τ<sub>s</sub> are the spin diffusion coefficient and spin diffusion time, respectively. The spins in the channel undergo a Larmor precession of frequency ω<sub>l</sub> = gμ<sub>B</sub>B<sub>⊥</sub>/ħ with Lande g-factor (g = 2) in the perpendicular magnetic field B<sub>⊥</sub>. From the fitting of Hanle curve labeled as (P-AP)/2 shown in Fig. 2(b), we get the effective polarization

Download English Version:

<https://daneshyari.com/en/article/7849083>

Download Persian Version:

<https://daneshyari.com/article/7849083>

[Daneshyari.com](https://daneshyari.com)